Received: 13 October 2017 | Revised: 9 November 2017 | Accepted: 14 November 2017

DOI: 10.1111/pce.13109

WILEY Plant, Cell & Environment

ORIGINAL ARTICLE

Impacts of long-term precipitation manipulation on hydraulic architecture and xylem anatomy of piñon and juniper in Southwest USA

P. J. Hudson[1] | J. M. Limousin[2] | D. J. Krofcheck[1] | A. L. Boutz[1] | R. E. Pangle[1] | N. Gehres[1] | N. G. McDowell[3] | W. T. Pockman[1]

[1] Department of Biology, MSC03 2020, University of New Mexico, Albuquerque, NM 87131-0001, USA

[2] Centre d'Ecologie Fonctionnelle et Evolutive CEFE, UMR5175, CNRS, Université de Montpellier, Université Paul-Valéry Montpellier, Montpellier 34293, France

[3] Earth Systems Analysis and Modeling, Pacific Northwest National Laboratory, Richland, WA 99352, USA

Correspondence
P. J. Hudson, Department of Biology, MSC03 2020, University of New Mexico, Albuquerque, NM 87131-0001, USA.
Email: phudson@unm.edu

Funding information
U.S. Department of Energy Office of Science (BER), Grant/Award Number: DE-FG02-07ER64393; National Science Foundation, Grant/Award Number: NSF DEB-0620482

Abstract

Hydraulic architecture imposes a fundamental control on water transport, underpinning plant productivity, and survival. The extent to which hydraulic architecture of mature trees acclimates to chronic drought is poorly understood, limiting accuracy in predictions of forest responses to future droughts. We measured seasonal shoot hydraulic performance for multiple years to assess xylem acclimation in mature piñon (*Pinus edulis*) and juniper (*Juniperus monosperma*) after 3+ years of precipitation manipulation. Our treatments consisted of water addition (+20% ambient precipitation), partial precipitation-exclusion (−45% ambient precipitation), and exclusion-structure control. Supplemental watering elevated leaf water potential, sapwood-area specific hydraulic conductivity, and leaf-area specific hydraulic conductivity relative to precipitation exclusion. Shifts in allocation of leaf area to sapwood area enhanced differences between irrigated and droughted K_L in piñon but not juniper. Piñon and juniper achieved similar K_L under ambient conditions, but juniper matched or outperformed piñon in all physiological measurements under both increased and decreased precipitation treatments. Embolism vulnerability and xylem anatomy were unaffected by treatments in either species. Absence of significant acclimation combined with inferior performance for both hydraulic transport and safety suggests piñon has greater risk of local extirpation if aridity increases as predicted in the southwestern USA.

KEYWORDS

drought, precipitation manipulation, water relations, xylem transport

1 | INTRODUCTION

Plant hydraulic architecture describes key aspects of xylem structure that predict plant function (Tyree & Ewer, 1991; Zimmerman, 1983). Comparative research has quantified the variation in hydraulic architecture among diverse taxa, revealing the correlation between vulnerability to embolism and local soil water potential (e.g., Choat et al., 2012; Maherali, Pockman, & Jackson, 2004; Pockman & Sperry, 2000). Parallel measurements have revealed that variation in other traits such as intrinsic xylem conductivity, stomatal regulation, and allocation of leaf area per unit sapwood area determine plant function over the operational range of xylem water potential (e.g., Martínez-Vilalta et al., 2009; Oren et al., 2002; Tyree & Ewer, 1991). Despite our knowledge of interspecific variation in hydraulic architecture and intraspecific differences among populations, the ability of individuals to modify hydraulic architecture in response to directional change or long-term fluctuation in climate drivers is poorly understood (Mencuccini, 2003).

Shifts in hydraulic architecture in response to environmental changes are potentially important because the expected response of long-lived species depends on whether hydraulic architecture is static or dynamically responsive to climate. In aridlands, altered precipitation regime and increased vapour pressure deficit as temperature increases are expected to increase the frequency and severity of drought in the next 50–100 years (Seager et al., 2007; Sheffield & Wood, 2007; Williams et al., 2013). Whether or not the hydraulic architecture and function of trees can change in response to fluctuating climate is difficult to investigate experimentally, but of great importance for

forecasting vegetation responses to climate change because current vegetation models treat hydraulic traits as static (Fisher et al., 2010; McDowell, 2011; McDowell et al., 2015; McMahon et al., 2011).

Intraspecific variation in hydraulic architecture, performance, and associated anatomy is well-established as growth conditions vary. Shoot level structural changes, such as decreases in leaf area that effectively increase leaf specific hydraulic conductance, coincide with reduced moisture availablity (Grier & Running, 1977; Mencuccini & Grace, 1994; Martínez-Vilalta & Piñol, 2002; Mencuccini, 2003; McDowell, Adams, Bailey, Hess, & Kolb, 2006; Martínez-Vilalta et al., 2009; Martin-StPaul et al., 2013). Embolism vulnerability decreases along moisture gradients or in contrasting environments, with relatively dry sites or drought treatments promoting increased resistance to loss of conductivity in both observational studies (Alder, Sperry, & Pockman, 1996; Barnard et al., 2011; Beikircher & Mayr, 2009; Corcuera, Cochard, Gil-Pelegrin, & Notivol, 2011; Herbette et al., 2010, Wortemann et al., 2011) and greenhouse experiments (Awad, Barigah, Badel, Cochard, & Herbette, 2010; Plavcova & Hacke, 2012; Stiller, 2009). Moreover, hydraulic transport capacity has been shown to decrease with reduced water availability or experimental drought (Fonti, Heller, Cherubini, Rigling, & Arend, 2012; Ladjal, Huc, & Ducrey, 2005; Maherali & DeLucia, 2000; Medeiros & Pockman, 2011), consistent with the proposed trade-off between hydraulic safety and efficiency (Tyree, Davis, & Cochard, 1994; Pockman & Sperry, 2000; Manzoni et al., 2013; but see Gleason et al., 2015). In response to drought, plants produce conducting elements with reduced lumen diameters, leading to reduction in hydraulically weighted lumen diameter (D_H as described in Pockman & Sperry, 2000; Sperry & Hacke, 2004; Beikircher & Mayr, 2009; Bryukhanova & Fonti, 2012; Fonti et al., 2012), and conducting efficiency, according to the Hagen–Poiseuille law (Tyree & Ewer, 1991; Zimmerman, 1983). Secondary cell wall thickness typically increases, resulting in enhanced conduit thickness to span ratio, an anatomical trait observed to closely correlate with embolism resistance [$(t/b)^2$, Hacke, Sperry, Pockman, Davis, & McCulloh, 2001; Pittermann, Sperry, Hacke, Wheeler, & Sikkema, 2006].

Do individuals of long-lived species modify hydraulic architecture in response to changing or fluctuating climate? Tree ring analyses suggest that aspects of secondary xylem anatomy reflect the climate of the growth year, with drier years producing smaller conduits (Zweifel, Zimmermann, Zeugin, & Newbury, 2006; Sterck, Zweifel, Sass-Klaassen, & Chowdhury, 2008; Fonti et al., 2012), as cell expansion depends on suitable turgor pressure and is impaired by drought (Hsiao & Acevedo, 1974; Sheriff & Whitehead, 1984). Accordingly, hydraulic transport capacity should be reduced when the hydroactive xylem reflects the accumulation of wood growth from multiple years of suboptimal climate (Bryukhanova & Fonti, 2012; Fonti et al., 2012). Ring-porous angiosperms exhibit a high degree of interannual plasticity in hydraulic performance and embolism vulnerability, with early-wood vessel diameter in *Quercus* species significantly correlated to spring temperature and precipitation, and current-year xylem dominating water transport (Zweifel et al., 2006; Fonti & García-González, 2008; Fonti et al., 2012). In contrast, effects of interannual plasticity may be muted in gymnosperms that maintain several years' worth of functional xylem because older xylem produced under more favourable conditions remains active (Sterck et al., 2008; Eilmann, Zweifel, Buchmann, Fonti, & Rigling, 2009).

Despite demonstrated intraspecific differences in hydraulic architecture between microsites, we lack empirical evidence of in situ adjustment of hydraulic architecture under altered water availability. In this study, our goal was to determine whether long-term precipitation manipulation promoted acclimation of xylem function in mature piñon-juniper woodland where the two dominant species operate at disparate positions along a plant functional continuum (McDowell et al., 2008). Piñon is relatively isohydric, maintaining leaf water potentials of approximately −2.5 MPa as soil moisture fluctuates, rapidly limiting transpiration, and thus carbon uptake, during drought. In contrast, juniper is relatively anisohydric, permitting leaf water potential to decline as soil dries, maintaining transpiration and carbon uptake over a larger range of soil moisture conditions (Klein, 2014; Limousin et al., 2013; Martínez-Vilalta, Poyatos, Aguadé, Retana, & Mencuccini, 2014; McDowell et al., 2008; Plaut et al., 2012; Skelton, West, & Dawson, 2015). We defined xylem hydraulic function in terms of intrinsic transport capability (sapwood-specific conductivity, K_S, $kg \cdot m^{-1} \cdot s^{-1} \cdot MPa^{-1}$), shoot-level hydraulic supply (leaf-specific conductivity, K_L, $g \cdot m^{-1} \cdot s^{-1} \cdot MPa^{-1}$), and vulnerability to embolism. We hypothesized that (a) K_S and K_L should vary in proportion to water availability, with higher K_S and K_L in irrigated individuals than those subjected to drought, (b) the consistent water potentials in isohydric piñon should promote little or no acclimation of embolism vulnerability across treatments, whereas the wide variation of water potential among treatments in anisohydric juniper should promote acclimation of hydraulic architecture relative to untreated controls such that embolism resistance increases with drought, and (c) changes in hydraulic transport efficiency and safety should correlate with shifts in anatomical structure.

2 | MATERIALS AND METHODS

2.1 | Study site

Our research used a rainfall manipulation experiment established in 2007 in a piñon-juniper woodland at the Sevilleta National Wildlife Refuge in central New Mexico, USA (34°23′11″ N, 106°31′46″ W, 1911 m; for details see Pangle, Hill, Plaut, Yepez, & Elliot, 2012; Plaut et al., 2012). Mean annual precipitation is 367.6 mm $year^{-1}$, with mean annual temperature of 12.7 °C, mean July maximum of 31.0 °C and mean December minimum of −3.3 °C (Moore, 2014). We established three replicate blocks of four treatments: ambient control (100% precipitation), irrigation (~130% precipitation), drought (~55% of ambient rainfall), and cover control (100% precipitation same coverage of inverted water troughs). Although shoot water potential measurements began in August 2007 (Pockman & McDowell, 2015), here, we use only data with concurrent hydraulic conductivity measurements (2010–2014). Due to complete piñon mortality in drought treatments of two replicate blocks in 2008, this study focused on the remaining block where target piñon trees persisted in the drought treatment. Branch samples collected for hydraulic conductivity measurements were harvested in June (premonsoon) and August (postmonsoon onset) of 2010, 2012, 2013, and 2014. Branch samples used for vulnerability curves were collected between August and November 2014.

2.2 | Shoot Ψ_W

We cut samples for predawn and midday water potential (hereafter, Ψ_{PD} and Ψ_{MD}) from each target tree between 0430 and 0545 hr and between 1200 and 1400 hr. Samples were stored in plastic bags with a scrap of moist paper towel to prevent desiccation, stored in shaded, insulated boxes before processing (between 15 and 60 min). Water potential (Ψ_W, MPa) was measured using a pressure chamber (PMS, Corvallis, OR).

2.3 | Hydraulic conductivity

Branches (~16 cm in length and 5–10 mm in diameter) cut from trees were sealed in humid plastic bags and transported to the laboratory where they were refrigerated until they were measured (within 24 hr). Before measurement, samples were submerged in 20 mM KCl solution and trimmed to ~4 cm in length, to remove distal embolized conduits. Samples were then inserted into a steady state flow meter to measure hydraulic conductance, K, kg·s^{-1}·MPa^{-1} (see Hudson, Razanatsoa, & Feild, 2009 and Feild et al., 2011 for full description of methods). The hydraulic head pressure was supplied by gas tank and maintained at 0.08 MPa, and we used degassed 20 mM KCl as a sap surrogate to control for ion-dependent effects on stem hydraulic function (Zwieniecki, Melcher, & Holbrook, 2001). We calculated stem hydraulic conductivity (Kh, kg·m·s^{-1}·MPa^{-1}) by multiplying K by sample length. Sapwood cross-sections were measured for each sample to normalize K_h at tissue level (K_S, sapwood-specific hydraulic conductivity, kg·m^{-1}·s^{-1}·MPa^{-1}). Sapwood area was measured from cross-sections taken at the sample distal end. Sections were stained with safaranin-O (0.01%) and photographed at 10× using a dissecting microscope (Carl Zeiss MicroImaging, Gottingen, Germany). We used ImageJ software (NIH Image, Bethesda, MD) to determine sapwood area (A_S) from images by subtracting pith area from cross-section area. Distal leaf area for each sample was used to normalize K_h at shoot level (K_L, leaf-specific hydraulic conductivity, g·m^{-1}·s^{-1}·MPa^{-1}). Projected leaf area (piñon) or photosynthetic stem area (juniper) was measured using a scanner and ImageJ software. To calculate A_S:A_L, sapwood area (m^2) was divided by leaf area (m^2) and multiplied by 10^4.

2.4 | Extending shoot hydraulic supply to predict transpiration

We derived branch-estimated transpiration (E_b, mmol·m^{-2}·s^{-1}) from a modified form of Darcy's Law (Manzoni et al., 2013; Tyree & Ewer, 1991):

$$E_b = \left(\frac{K}{A_L}\right)\Delta\Psi,$$

where K is branch conductance (mmol·s^{-1}·MPa^{-1}, derived by dividing K by molar mass of water), A_L is branch leaf area (m^2), and $\Delta\Psi$ is the driving gradient for water transport (Ψ_{PD}–Ψ_{MD}, MPa). E_b is in the same units as transpiration measured by portable leaf level gas exchange equipment and represents a point measurement similar to that described by Wullschleger, Meinzer, and Vertessy (1998). E_b will over estimate actual transpiration, because it cannot account for resistances imposed by extraxylary transport, mesophyll conductance, stomatal conductance, or boundary layer conductance, all of which will reduce water transport through leaf tissue relative to shoot xylem.

2.5 | Vulnerability to embolism

We measured embolism vulnerability of branches (~30 cm in length and 8–12 mm in diameter) cut from trees under water, transferred to water-filled containers, and allowed to rehydrate in a refrigerator or under vacuum infiltration overnight or until measurement within 48 hr of collection. Rehydrated branches had indistinguishable K_S compared to vacuum infiltrated branches (p = .5 for piñon, p = .61 for juniper), so we switched to rehydration refilling as it allowed for more rapid sample processing. Prior to measurement, we trimmed samples while submerged in 20 mM KCl solution. Hydraulic conductivity was measured as above, with the initial K_h value designated K_{max}. After K_{max} was established, the sample was placed in a double-ended pressure sleeve, and the air injection technique (Sperry & Saliendra, 1994) was used to generate embolism-propagating stress. Pressurization lasted 2 min, and samples were depressurized slowly (~2 MPa min). We established that pressurization for 2 min resulted in similar loss of conductivity observed with longer (5 or 10 min) treatment (data not shown). Samples were allowed to equilibrate following depressurization and then reconnected to the steady state flow meter to measure K. Percent loss of conductivity (PLC) was calculated as:

$$PLC = 100 \cdot \left(1 - \frac{K_i}{K_{max}}\right),$$

where K_i is the measurement of K after the ith pressurization. Five or six pressurizations were carried out on each sample, depending on species. Juniper samples were pressurized over a span of 1.5–14 MPa, whereas piñon samples were pressurized over a span of 1.5–6 MPa.

We used a Weibull function to generate vulnerability curves using PLC data points (Neufeld et al., 1992). A Weibull function was preferred over a sigmoid function because a Weibull forces the vulnerability curve to start at the origin (i.e., 0 stress results in 0 PLC). The structure of the Weibull function is

$$PLC = 100 - 100 \cdot e^{\left[-\left(\frac{\Psi_W}{a}\right)^b\right]},$$

where a and b are curve fitting parameters (Hubbard, Ryan, Stiller, & Sperry, 2001). Parameters a and b were subsequently used to calculate P_{50} from the Weibull fit, according to the equation:

$$P_{50} = a \cdot \sqrt[b]{-1n(.5)}.$$

The derivative of the Weibull function at P_{50} was then used to find the slope of the line tangent to P_{50}. The x-intercept of this line is P_e, the air entry threshold (Domec & Gartner, 2001), and the x-value when y = 100 is P_{max}, the hydraulic failure threshold. The difference between P_e and P_{max} is the drought stress interval (MPa) and represents the span of water potentials over which a plant experiences drought stress but maintains some degree of hydraulic function.

2.6 | Wood anatomy

Hand sections were obtained from vulnerability curve samples, stained with Safranin-O, and photographed at 400× on a compound microscope (Zeiss AxioImager M1, Zeiss). Only earlywood tracheids from recent growth (i.e., 2014) were measured, as these tracheids are responsible for the majority of water transport (Bouche et al., 2014; Domec & Gartner, 2002). Lumen area and adjacent anticlinal wall thickness (T_W) were traced using ImageJ. Lumen diameters (D) were calculated as the square root of lumen area, which is more appropriate for rectilinear tracheids (Hacke, Sperry, & Pittermann, 2004; Sperry & Hacke, 2004). A minimum of 20 tracheids from each sample were measured, for N = 300 tracheids per species, per treatment. We confirmed that cross-section lumen diameter distributions were similar to those measured in macerated samples. The hydraulically weighted lumen diameter (D_H) was calculated as:

$$D_H = 2\left(\frac{\Sigma r^5}{\Sigma r^4}\right),$$

where r is the lumen radius, in microns (Sperry & Hacke, 2004). Conduit thickness to span ratio $(T_W/D)^2$ was calculated as the square of the ratio of adjacent double wall thickness to lumen diameter (Hacke et al., 2001).

2.7 | Wood density

Wood density (ρ_W, g cm^{-3}) was measured by volumetric displacement. A small piece of branch, immediately adjacent to the K_h sample, was stripped of bark, split along the long axis, and stripped of pith. One of the halves was shortened, to aid in subsample identification. Each subsample was submerged in a beaker of water on a scale. The resulting mass change caused by the subsample is equal to volume of water displaced; mass was converted to volume by dividing by the density of water at standard temperature and pressure (1 g cm^{-3}). The mass of paired subsamples was determined after drying in a coin envelope for 48 hr at 60 °C. ρ_W is calculated as dry mass divided by fresh volume (McCulloh, Johnson, Meinzer, & Woodruff, 2014).

2.8 | Data analysis

We used R (R Core Team, 2013) and the packages lme4 (Bates, Maechler, & Bolker, 2012) and nlme (Pinheiro, Bates, DebRoy, & Sarkar, 2016) to perform linear mixed effects analyses of the relationship between our physiological response variables and drought imposition both before and after monsoon precipitation input. We set treatment, period (before or after monsoon onset), and the interaction term as fixed effects. As random effects, we structured the model to allow for random intercepts for individual trees and sampling dates. Separate models for pre- and postmonsoon data were generated if the full model indicated a significant period effect. When visual inspection of residual plots revealed obvious deviations from homoscedasticity or normality (Winter, 2013), square root or natural log transformations were employed to meet necessary model assumptions. P values were obtained by likelihood ratio tests of the full model with the effect in question against the model without the effect in question. We also composed models that used the interaction of experimental day and treatment as a fixed effect, with target tree as a random effect. This model structure allowed us to identify sampling dates where water status or hydraulic function differed significantly across treatments within species. Reported values of water potential and hydraulic conductivity are the least squares mean estimates ± modeled standard error.

Covariation of water stress, hydraulic function, treatment, and period were also assessed using linear mixed effects models. We examined the relationships of K_S, K_L, and E_b to Ψ_{PD}, which we used as a proxy for water stress intensity. For response variables where Ψ_{PD} was determined to be a significant fixed effect, but treatment was not, data were pooled, and a post hoc linear regression was used to determine the significance and strength of the relationship between water stress and hydraulic function. Reported coefficients (intercepts and slopes) are the least squares mean estimates ± modeled standard error.

We used a multivariate analysis of variance (MANOVA) framework to detect significant differences in vulnerability to embolism and tracheid anatomy due to treatment and species. Subsequent comparisons of means (univariate analysis of variance (ANOVA) with Tukey's honest significant difference (HSD) comparisons of means) were conducted if significant treatment effects were discovered. Data were analyzed in R, and all values presented are mean ± standard error.

3 | RESULTS

3.1 | Climate and treatment effects on plant water status

Precipitation inputs to the various treatments over the 3 years preceding our measurements totaled 1,110.9, 982.4, and 637.6 mm for irrigation, control, and drought, respectively. During the measurement years, ambient annual precipitation ranged from a minimum of 252 mm in 2011 to a maximum of 385.8 mm in 2013 (Figure 1a) and averaged 304.2 (±1 SE = 23.1) mm yr^{-1}, which was less than the 20-year mean reported from a nearby Long-Term Ecological Research (LTER) meteorological station (362.7 mm yr^{-1}, 1989–2009, Cerro Montosa #42; http://sev.lternet.edu/). We estimated precipitation for drought and irrigation plots using the known percentage rainout coverage of each drought plot and the volume of water added to irrigation plots (Pangle et al., 2012). Supplemental water addition elevated irrigation precipitation inputs to 411.7 ± 27.7 mm yr^{-1}, from 2010 to 2014, which was 21.1% greater than ambient (average irrigation was 81.8 ± 4.3 mm yr^{-1}, Figure 1a,b). Based on projected 45% precipitation reduction, drought treatment annual precipitation was calculated to be 162.7 ± 12.7 mm yr^{-1} for years 2010 to 2014 (Figure 1b).

Plant water status of piñon and juniper, as measured by predawn water potential, was strongly affected by our treatments (Figure 2a, b). As expected, irrigation had a stronger effect on plant water status during the spring dry period, whereas drought structures had a stronger effect during summer monsoon. Piñon water status responded more strongly to water addition, whereas juniper water status responded more strongly to water withholding. Before the monsoon, our irrigation treatments raised Ψ_{PD} by 0.59 (24.5%) and 0.58 MPa (16.2%) for piñon and juniper, respectively, relative to ambient conditions. Following the monsoon, drought structures decreased Ψ_{PD} by

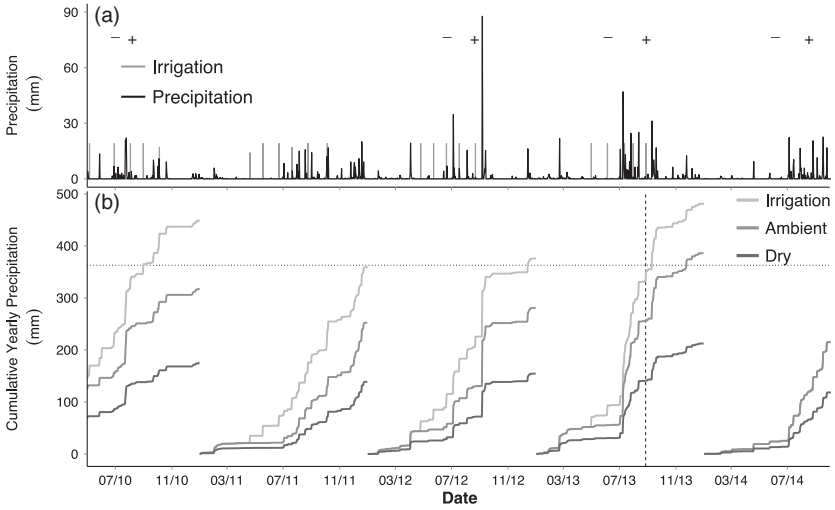

FIGURE 1 Absolute (a) and cumulative yearly (b) precipitation and irrigation inputs on experimental plots from May 1st 2010 to October 1st 2014. In (a), black vertical lines indicate precipitation events, gray vertical lines represent irrigation treatment supplemental watering. Premonsoon sampling dates are denoted by −, postmonsoon onset sampling dates are denoted by +. Solid lines in (b) represent treatment cumulative yearly water inputs, the horizontal dotted line represents the 20-year average (362.7 mm yr^{-1}, 1989–2009) from the nearest site meteorological station, and the vertical dashed line denotes the last supplemental watering; after this date, ambient and irrigation treatments received identical precipitation inputs

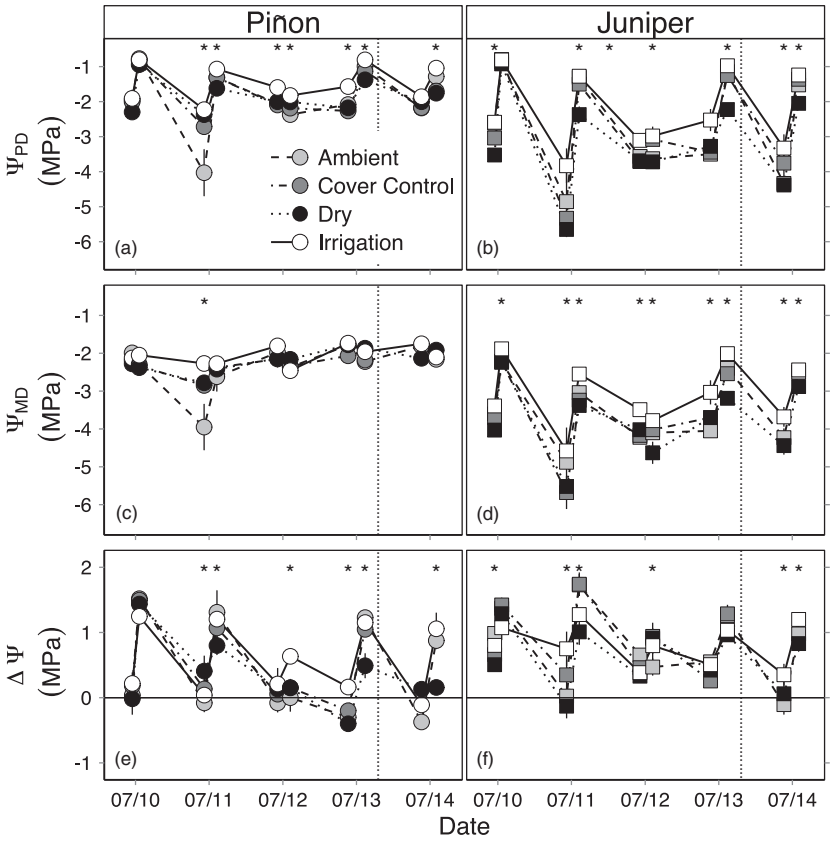

FIGURE 2 Mean predawn water potential (Ψ_{PD}), midday water potential (Ψ_{MD}), and driving gradient ($\Delta\Psi$) of pre- and postmonsoon onset sampling of piñon (a, c, and e) and juniper (b, d, and f) from June 2010 through August 2014. Circles represent piñon means, and squares represent juniper means. Error bars are ±1 SE. Asterisks indicate significant treatment effects for a given sampling date ($p < .05$). Supplemental water addition ended in 2013, as did midday cover control measurements and is indicated by the vertical dotted line

0.2 (15.5%) and 0.59 MPa (37.6%) for piñon and juniper, respectively, relative to ambient conditions. For both species, irrigation elevated Ψ_{PD} relative to all other treatments before monsoon onset, whereas ambient Ψ_{PD} did not differ from drought treatment (Figure 3a). In all treatments, we observed higher Ψ_{PD} for piñon compared to juniper. After monsoon onset, irrigated piñon continued to have higher Ψ_{PD} than all other treatments, but Ψ_{PD} in irrigated juniper was no longer distinct from cover control juniper. Drought Ψ_{PD} was lowered relative to ambient treatment for both species. After the start of the monsoon, piñon Ψ_{PD} was only higher than juniper in the water addition and water withholding treatments (Figure 3a).

Piñon Ψ_{MD} converged on −2.2 MPa (Figure 2c), both pre- and postmonsoon, although irrigated individuals had higher Ψ_{MD} compared to all other treatments before the monsoon (Figure 3b). Though broadly consistent with isohydric Ψ_W regulation, during the particularly dry 2011 premonsoon sampling period, ambient treatment piñon Ψ_{PD} (−4.03 ± 0.67) and Ψ_{MD} (−3.95 ± 0.61 MPa) fell below the isohydric threshold reported at this site and in the literature (e.g., Breshears et al., 2009; Limousin et al., 2013; McDowell et al., 2008; Pangle et al., 2015; Plaut et al., 2012; West, Hultine, Jackson, & Ehleringer, 2007). Before the monsoon, nonirrigated juniper also converged on a common Ψ_{MD} (~−4.2 MPa, Figure 2d), though irrigated trees had higher water status. After the

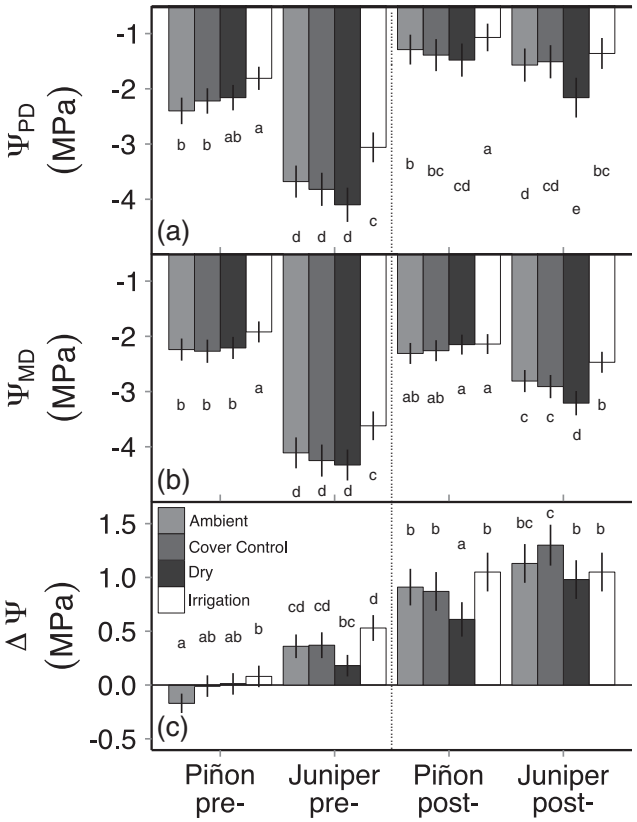

FIGURE 3 Linear mixed effects model means of (a) predawn water potential (Ψ_{PD}), (b) midday water potential (Ψ_{MD}), and (c) driving gradient for transpiration ($\Delta\Psi$) for pre- and postmonsoon onset sampling of piñon and juniper. Letters indicate differences significant at $p < .05$, and comparisons are restricted to within sampling period, between species and across treatments. Error bars are ±1 SE

monsoon began, irrigated juniper Ψ_{MD} was higher than ambient and cover control, which was in turn higher than drought Ψ_{MD} (Figure 3b). Minimum juniper Ψ_{PD} (−5.65 ± 0.17) and Ψ_{MD} (−5.68 ± 0.44 MPa) occurred in drought and cover control during the hot dry premonsoon period of 2011.

Driving gradient for transpiration ($\Delta\Psi$, MPa) was impacted by treatment for both species (Figures 2e,f). Prior to monsoon activity, irrigation increased $\Delta\Psi$ above all other treatments for piñon, whereas only irrigation and drought treatments differed for juniper (Figure 3c). After the monsoon, drought treatment had reduced $\Delta\Psi$ compared to all other treatments for piñon, whereas cover control treatment had elevated $\Delta\Psi$ compared to both drought and irrigation treatments for juniper. Interestingly, $\Delta\Psi$ was not different between species in either the ambient or irrigation treatments but was lower for piñon in the drought and cover control treatments.

Ψ_{PD} strongly predicted Ψ_{MD} for both species ($p < .0001$) before the monsoon, but the relationship was stronger in anisohydric juniper ($R^2 = 0.89$) than isohydric piñon ($R^2 = 0.67$, Figure S1a). After the monsoon, Ψ_{PD} continued to be a strong predictor of Ψ_{MD} ($R^2 = 0.81$) in juniper but ceased to have a significant relationship in piñon ($R^2 = 0.02$, Figure S1c). Consequently, the power of Ψ_{PD} to predict $\Delta\Psi$ shifted from weak ($R^2 = 0.07$) to strong ($R^2 = 0.67$) with monsoon onset in piñon, whereas this linear relationship remained consistent and moderate in juniper ($R^2 = 0.39$ pre-, $R^2 = 0.31$ postmonsoon, Figure S1b,d). No treatment effects were found for these relationships in either species.

3.2 | Shoot level hydraulic architecture

Variation in long-term moisture availability yielded differences in allocation ratios of sapwood area to leaf area (Figure 4a). Irrigated piñon reduced A_S:A_L relative to ambient ($p = .0003$) and droughted ($p = .02$) piñon, but droughted piñon did not increase A_S:A_L relative to ambient ($p = .2$, Figure 5a). Patterns of tissue allocation in response to precipitation manipulation were less clear for juniper (Figure 4b). Drought and cover control treatments had increased A_S:A_L relative to ambient ($p = .023$ and $p = .007$, respectively), whereas irrigated trees only reduced A_S:A_L compared to cover control ($p = .018$, Figure 5a). Between species, piñon and juniper maintained similar A_S:A_L values in all treatments, except ambient, wherein piñon had higher A_S:A_L than juniper ($p = .009$, Figure 5a).

between pre-/postmonsoon sampling dates, yet we found K_S increased with increasing moisture availability in both species, and dynamics of treatment effects varied by species (Figure 5b). Irrigated piñon displayed a higher K_S than all other treatments ($p < .0001$ for all comparisons), which did not differ from one another. In contrast, irrigated juniper deviated from droughted and ambient juniper ($p = .007$ and $p = .04$, respectively) but not cover control. Juniper K_S was greater than piñon in all treatments but only significantly different in the drought and cover control treatments ($p = .04$ and $p = .0003$, respectively).

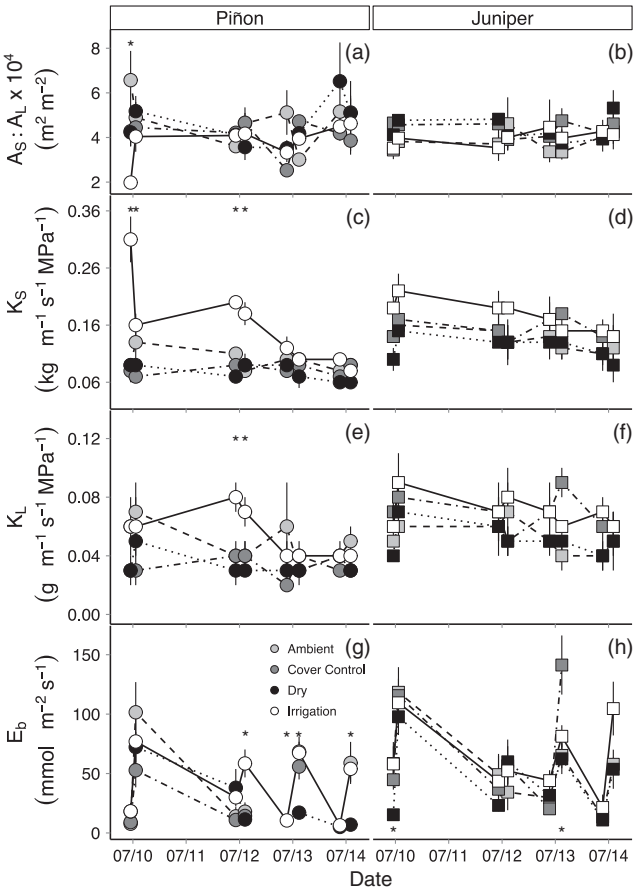

FIGURE 4 Mean (a and b) sapwood area to leaf area ratio (A_S:A_L); (c and d) sapwood-specific hydraulic conductivity (K_S); (e and f) leaf-specific hydraulic conductivity (K_L); and (g and h) branch estimated transpiration (E_b) for piñon (a, c, e, and g) and juniper (b, d, f, and h) from each sampling date. Error bars are ±1 SE. Asterisks indicate significant treatment effects for a given sampling date ($p < .05$)

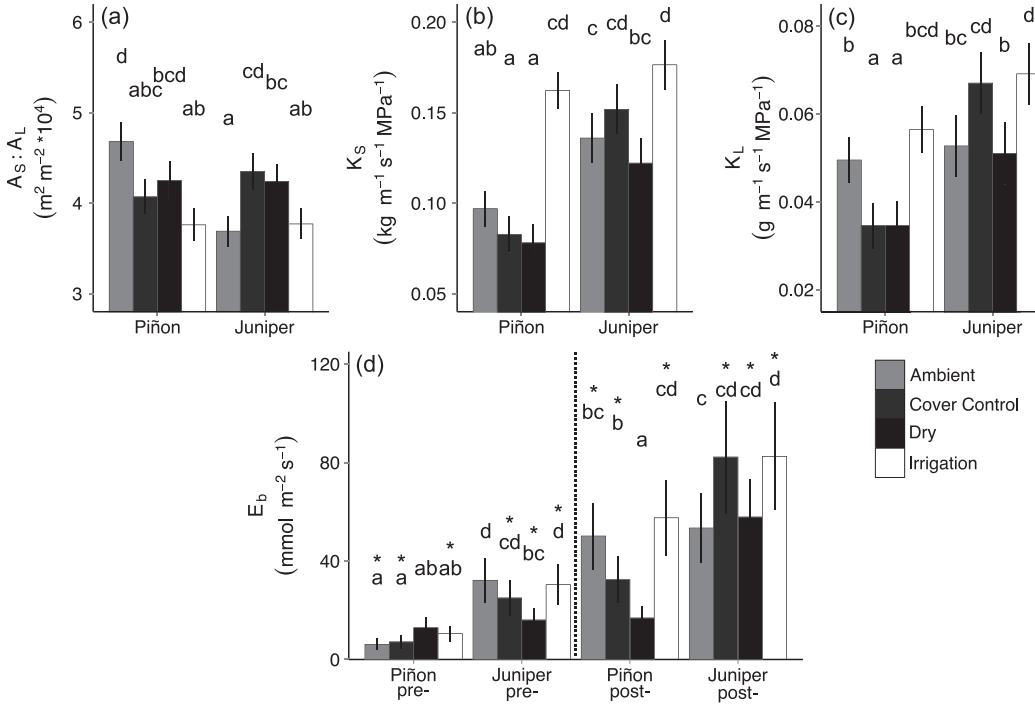

FIGURE 5 Linear mixed effects model means of (a) sapwood area to leaf area ratio (A_S:A_L), (b) sapwood-specific hydraulic conductivity (K_S), (c) leaf-specific hydraulic conductivity (K_L), and (d) branch estimated transpiration (E_b) by species and treatment over study duration. Error bars ±1 SE, and different letters indicate significant differences at $p \leq .05$. In (d), comparisons between treatments and species are displayed by season (pre-/postmonsoon onset, separated by vertical dotted line), and asterisks indicate significant season effects within treatment and species

Experimental treatments influenced shoot level hydraulic supply (Figure 4e,f). As with K_S, K_L was not affected by pre-/post-monsoon changes in precipitation but did scale with treatment water availability. Ambient and irrigated piñon had higher K_L than cover control and drought piñon ($p < .03$, Figure 5c). Irrigated juniper had higher K_L than drought juniper ($p = .04$), though neither treatment deviated significantly from ambient. Between species, K_S and A_S:A_L varied such that in ambient conditions, piñon and juniper achieved similar rates of K_L ($p = .8$, Table 2). However, in both water addition and water withholding treatments, juniper achieved higher K_L than piñon ($p < .02$, Figure 5c).

Branch estimated transpiration responded to monsoon precipitation, and we observed season by treatment interaction effects (Figures 4g,h and 5d). E_b did not vary in piñon across treatments premonsoon ($p > .05$). Experimental drought suppressed E_b in piñon relative to all other treatments after monsoon onset ($p > .05$), whereas water addition elevated E_b compared to cover control ($p = .047$) but not ambient piñon ($p = .470$). Droughted juniper had lower E_b than ambient and irrigation treatments before monsoon onset ($p < .01$). Monsoon precipitation raised E_b in all experimental treatments ($p \geq .05$) but not ambient ($p = .16$), and only ambient and irrigation treatments deviated from each other ($p = .03$). Prior to the monsoon, piñon had lower E_b than juniper in all treatments except drought ($p < .004$), but after monsoon onset, piñon and juniper achieved equivalent E_b in irrigation and ambient treatments ($p > .2$).

3.3 | Relationships between water stress and hydraulic performance

We found no relationship between Ψ_{PD} and K_S ($p = .43$ and $p = .21$ for piñon and juniper, respectively, Table 1, Figure 6a, and Table S1) or K_L ($p = .21$ and $p = .07$ for piñon and juniper, respectively, Table 1, Figure 6b, and Table S2). Ψ_{PD} covaried with E_b (Table 1, Figure 6c, and Table S3), and after linear mixed effects models failed to reveal significant differences in the relationship across treatments within piñon ($p = .47$) or juniper ($p = .17$), we pooled the treatment data for both species. Ψ_{PD} explained similar proportions of variation in E_b for both species (piñon $R^2 = 0.41$, juniper $R^2 = 0.45$). Model slopes and intercepts were used to estimate Ψ_{PD} at zero E_b (referred to hereafter as $\Psi_{E=0}$), the point at which stomata remain closed and transpiration is zero. Our estimates of $\Psi_{E=0}$ in piñon (−2.34 ± 0.09 MPa) and juniper (−4.86 ± 0.19 MPa) were consistent with their isohydric and anisohydric stomatal regulation, respectively.

3.4 | Vulnerability to embolism and hydraulic decline

Embolism vulnerability did not vary among treatments in either species ($p = .45$ for piñon, $p = .83$ for juniper, Figure 7a), so we pooled species data to generate composite curves. Piñon was significantly more vulnerable to embolism than juniper. For the four curve parameters calculated (P_e, P_{50}, P_{max}, and drought stress interval), piñon values were roughly half as large as juniper (Table 2). Plotting the decline of K_S with increasing simulated drought stress (Figure 7b) showed that juniper possessed greater rehydrated maximum K_S compared to piñon ($p = .0009$). Maximum K_S was nearly twice as large as native K_S for all treatments in juniper (one sample t-test, $p < .03$) but did not differ in piñon ($p > .4$).

3.5 | Anatomical structure and wood density

Earlywood tracheids were structurally similar in both species across all treatments (Figure 8). Compared to juniper in the same treatment,

TABLE 1 Coefficients ± standard error of the linear mixed effects model regressions between Ψ_{PD} (MPa) and K_S ($kg \cdot m^{-1} \cdot s^{-1} \cdot MPa^{-1}$), K_L ($g \cdot m^{-1} \cdot s^{-1} \cdot MPa^{-1}$), and E_b ($mmol \cdot m^{-2} \cdot s^{-1}$). Response variable data were log transformed as necessary to meet assumptions of normality. *p* values for ambient treatments indicate significance of relationship between response variable and Ψ_{PD}; all other *p* values indicate significance of difference between treatment slopes and ambient control slope

K_S					
Species	Treatment	Intercept	Slope	R^2	*p* value
Piñon					
	Ambient	0.12 ± 0.02	0.014 ± 0.013	—	.26[a]
	Cover control	0.08 ± 0.03	−0.002 ± 0.018	—	.38[a]
	Dry	0.08 ± 0.04	−0.003 ± 0.021	—	.43[a]
	Irrigation	0.07 ± 0.03	−0.067 ± 0.020	—	.0001[b]
	Model: lme(K_S ~ Ψ_{PD} * treatment, na.action = na.omit, method = "ML")				
Juniper					
	Ambient	0.14 ± 0.02	0.003 ± 0.006	—	.56[a]
	Cover control	0.17 ± 0.03	0.009 ± 0.008	—	.51[a]
	Dry	0.14 ± 0.03	0.004 ± 0.009	—	.90[a]
	Irrigation	0.17 ± 0.03	−0.002 ± 0.009	—	.57[a]
	Model: lme(K_S ~ Ψ_{PD} * treatment, na.action = na.omit, method = "ML")				
K_L					
Piñon					
	Ambient	0.061 ± 0.010	0.007 ± 0.005	—	.20[a]
	Cover control	0.038 ± 0.015	0.002 ± 0.008	—	.54[a]
	Dry	0.049 ± 0.017	0.008 ± 0.009	—	.92[a]
	Irrigation	0.041 ± 0.014	−0.011 ± 0.008	—	.03[b]
	Model: lme(K_L ~ Ψ_{PD} * treatment, na.action = na.omit, method = "ML")				
Juniper					
	Ambient	0.053 ± 0.010	−0.00006 ± 0.005	—	.99[a]
	Cover control	0.080 ± 0.015	0.0052 ± 0.008	—	.27[a]
	Dry	0.067 ± 0.016	0.0054 ± 0.009	—	.27[a]
	Irrigation	0.069 ± 0.015	0.00001 ± 0.008	—	.99[a]
	Model: lme(K_L ~ Ψ_{PD} * treatment, na.action = na.omit, method = "ML")				
E_B					
Piñon					
	Ambient	130.76 ± 16.02	56.78 ± 10.29	—	<.0001[a]
	Cover control	91.23 ± 25.31	40.06 ± 16.79	—	.32[a]
	Dry	115.81 ± 27.37	53.59 ± 16.62	—	.85[a]
	Irrigation	98.81 ± 22.65	38.03 ± 15.04	—	.22[a]
	All treatments	**109.68 ± 9.02**	**47.46 ± 6.02**	**0.41**	**<.0001**
	Model: lme(E_b ~ Ψ_{PD} * period, na.action = na.omit, method = "ML")				

(Continues)

TABLE 1 (Continued)

K_S					
Juniper					
	Ambient	108.98 ± 12.33	20.71 ± 4.63	–	<.0001[a]
	Cover control	161.06 ± 18.81	35.48 ± 6.94	–	.036[b]
	Dry	107.60 ± 19.64	21.16 ± 6.87	–	.95[a]
	Irrigation	124.71 ± 17.29	27.46 ± 6.82	–	.32[a]
	All treatments	**124.42 ± 6.71**	**25.83 ± 2.47**	**0.45**	**<.0001**
	Model: lme(E_B ~ Ψ_{PD} * period, na.action = na.omit, method = "ML")				

Bold font signifies the statistical analysis of pooled treatment data.

Superscripted letters signify statistical distinctions between treatments.

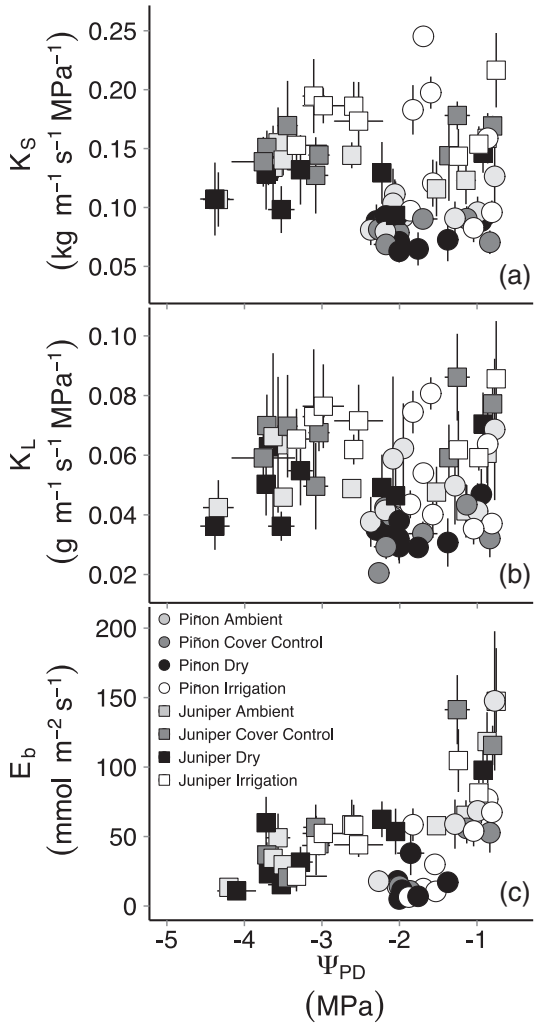

FIGURE 6 Relationships between predawn water potential (Ψ_{PD}) and (a) sapwood-specific hydraulic conductivity (K_S), (b) leaf-specific hydraulic conductivity (K_L), and (c) branch estimated transpiration (E_b). Error bars are ±1 SE; data from all years are pooled

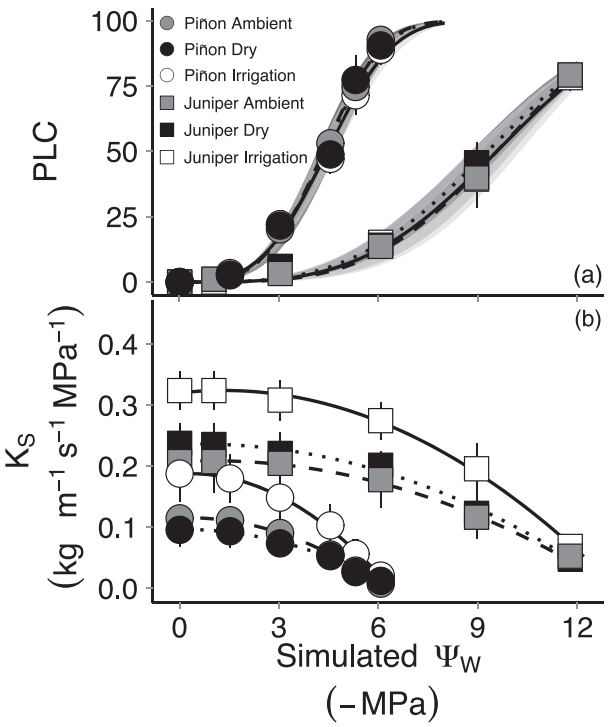

FIGURE 7 Treatment specific relationships between air-injection simulated water potential and (a) percent loss conductivity and (b) absolute decline in sapwood-specific hydraulic conductivity (K_S) for piñon (circles) and juniper (squares) sampled in 2014. Solid lines denote irrigation fits, dashed lines denote ambient control fits, and dotted lines denote drought treatment fits. Shaded regions about the vulnerability curves in (a) are minimum/maximum vulnerability curves based on mean PLC ± 1 SE for each treatment, within each species

piñon tracheids tended to have larger lumens and slightly, though not significantly, higher D_H, with the exception that droughted piñon had a significantly higher D_H than droughted juniper (Figure 8a). We detected no differences in double wall thickness (T_W) across treatments or between species (Figure 8b). The combination of similar T_W and reduced D_H in juniper led to a significantly greater thickness to span ratio $[(T_W/D)^2]$ compared to piñon in all treatments (Figure 8c), which is consistent with the reported relationship between embolism resistance and $(T_W/D)^2$ (Bouche et al., 2014; Hacke et al., 2001). Multivariate analysis of variance did not detect significant differences in tracheid anatomy across treatments in piñon (p = .91) or juniper (p = .44). Wood density did not differ significantly between species or across treatments (Figure 8d).

TABLE 2 Parameters extracted from vulnerability curves. Letters denote significant differences between species and across treatments ($p \leq .05$)

Species	Treatment	P_e (−MPa)	P_{50} (−MPa)	P_{max} (−MPa)	DSI (MPa)
Piñon					
	Ambient	2.59 ± 0.07[a]	4.36 ± 0.1[a]	6.13 ± 0.22[a]	3.53 ± 0.26[a]
	Dry	2.60 ± 0.28[a]	4.43 ± 0.19[a]	6.24 ± 0.54[a]	3.64 ± 0.78[a]
	Irrigation	2.56 ± 0.27[a]	4.48 ± 0.22[a]	6.41 ± 0.39[a]	3.84 ± 0.5[a]
	Pooled	2.55	4.39	6.24	3.69
Juniper					
	Ambient	5.34 ± 0.14[b]	9.39 ± 0.43[b]	13.44 ± 0.73[b]	8.09 ± 0.61[b]
	Dry	5.65 ± 0.73[b]	9.29 ± 0.44[b]	12.93 ± 0.52[b]	7.28 ± 0.93[b]
	Irrigation	6.13 ± 1.05[b]	9.53 ± 0.67[b]	12.92 ± 0.63[b]	6.79 ± 1.09[b]
	Pooled	5.58	9.46	13.35	7.77

Note. DSI = drought stress interval.

Superscripted letters signify statistical distinctions between treatments.

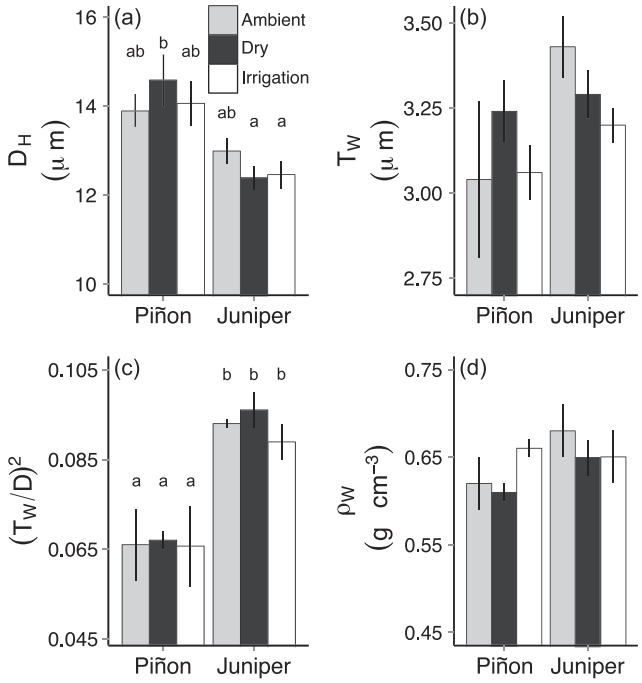

FIGURE 8 Barplots for tracheid anatomy and wood density measurements from piñon (N = 3 per treatment) and juniper (N = 3 or 5 per treatment) vulnerability curve samples collected in 2014. Parameters shown are (a) tracheid hydraulically weighted lumen diameter (D_H), (b) tracheid double wall thickness (T_W), (c) tracheid thickness to span ratio [$(T_W/D)^2$], and (d) wood density (ρ_W). Bars labeled with different letters are significantly different as determined by *post hoc* Tukey's honest significant difference tests at 95% confidence level

4 | DISCUSSION

4.1 | Acclimation responses to altered precipitation regimes

Despite the sustained and significant effects of our treatments on plant water status (Figures 1 and 2), we observed only limited evidence of species-specific acclimation in hydraulic architecture. Although irrigated piñon increased investment in leaf area (decreased A_S:A_L), the concomitant increase in K_S yielded similar K_L to ambient trees (Figures 4 and 5). The combination of similar tracheid D_H (Figure 8), increased Ψ_{PD} (Figure 3) and reduced PLC (Figure 9), suggests that increased K_S in irrigated trees was due to decreased embolism formation rather than enhanced intrinsic xylem conductivity through adjustments in tracheid dimensions. Ultimately, the irrigation response in piñon was to add leaves in proportion to shoot hydraulic conductivity rather than enhance shoot hydraulic conductivity.

The increased K_S in irrigated versus ambient juniper, in the absence of adjustment of A_S:A_L across treatments, suggests increased water availability induced a modest increase in xylem conducting efficiency. Embolism formation, predicted to be minimal in both treatments (maximum PLC < 12%, Figure 7), is unlikely to have contributed to this result. Yet earlywood D_H was also consistent across treatments (Figure 8), implying that changes in conducting efficiency occurred via changes at the level of pit structure.

Although irrigation led to shoot-level responses, after more than 6 years of decreased moisture availability, the only significant response observed was a reduction of leaf area relative to sapwood area in juniper (Figure 5a). The similarity in maximum premonsoon water stress in ambient and drought treatments for both species (Figure 3), coupled with unchanged embolism vulnerability (Figure 6), suggests similar drought impacts for these two treatments (Figure 9). Droughted piñon had reduced K_L compared to ambient piñon (Figure 5c) but similar embolism resistance (Figure 6, Table 2), which indicates piñon have minimal ability to compensate for chronic water shortage. The drought treatment reduction in K_L may be attributable to reduced ability to repair embolism via impaired phloem function due to insufficient hydration (Nardini, Lo Gullo, & Salleo, 2011; Sevanto, 2014) or reduced proportion of viable cross-sectional area. In contrast, droughted juniper maintained similar K_L as in ambient juniper by reducing leaf area relative to sapwood area (Figure 5c), demonstrating a homeostatic mechanism for maintaining hydraulic supply to photosynthetic tissue when challenged by chronic water shortage (Mencuccini & Grace, 1994; McDowell et al., 2006; Martínez-Vilalta et al., 2009; Martin-StPaul et al., 2013). The low predicted PLC values in both drought and ambient treatments (Figure 9) suggest that mechanisms responsible for leaf area reduction observed in juniper must operate at relatively low predicted loss of shoot xylem hydraulic conductivity.

The absence of significant shifts in embolism vulnerability (Figure 6) and earlywood tracheid anatomy (T_W, D_H, and $(T_W/D)^2$; Figure 8) in

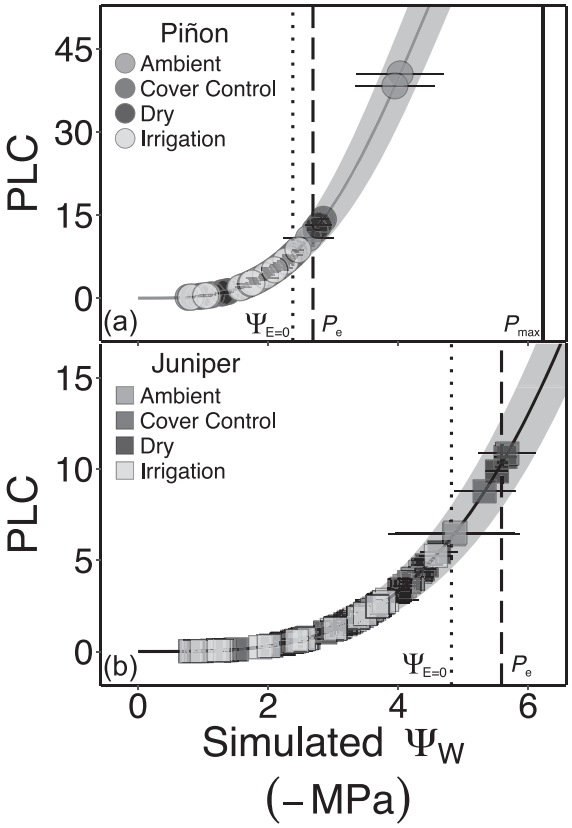

FIGURE 9 Predicted percent loss of conductivity based on mean water status for piñon (circles, a) and juniper (squares, b). Horizontal error bars are ±1 SE. Vulnerability curves are composites based on pooled species data, and the shaded areas about the curves represent min/max curves based on ±1 SE from mean PLC. Dot-dash vertical lines indicate Ψ_{PD} of zero transpiration ($\Psi_{E=0}$), dotted vertical lines indicate P_e (drought stress onset), and the solid vertical line in (a) represents P_{max} (hydraulic failure threshold)

either species supports the hypothesis that mature trees have little ability to modify embolism vulnerability. Limited adjustment in hydraulic architecture has been observed in other conifers (Mencuccini & Comstock, 1997; Martínez-Vilalta & Piñol, 2002; Martínez-Vilalta et al., 2009; Corcuera et al., 2011; Lamy et al., 2011; Klein, Di Matteo, Rotenberg, Cohen, & Yakir, 2013; Lamy et al., 2013). Importantly, this finding suggests that, unlike developmental differences between individuals in different microsites, acclimation of aerial tissues in established individuals will not contribute to the climate change responses of widespread coniferous biomes such as piñon-juniper woodland.

4.2 | Relative performance of piñon and juniper

Our observations that juniper, the more drought-tolerant species (Limousin et al., 2013; Linton, Sperry, & Williams, 1998; McDowell et al., 2008; Pangle et al., 2015; Plaut et al., 2012; West et al., 2007), matched or exceeded piñon performance in all measured hydraulic metrics which does not support the proposed hydraulic efficiency versus safety tradeoff (as discussed in Tyree, Davis, & Cochard, 1994). The comparable K_S and superior embolism resistance of juniper to piñon were also surprising because wood density did not vary between species. Wood density, which is expected to reflect the carbon cost associated with secondary cell wall lignification (Pittermann, Sperry, Wheeler, Hacke, & Sikkema, 2006), is often negatively correlated with K_S and K_L (Bucci et al., 2004; Meinzer et al., 2008) and positively correlated with embolism resistance (Hacke et al., 2001; Hacke & Jansen, 2009; Meinzer, Johnson, Lachenbruch, McCulloh, & Woodruff, 2009). Because juniper routinely exhibits more negative water potentials than piñon (Figures 2 and 3) and is much more resistant to embolism formation and spread (Figure 9), we predicted that juniper xylem would have increased wood density due to enhanced lignification of tracheid secondary walls. The similarity between piñon and juniper earlywood tracheids (Figure 8) defied this prediction. Earlywood tracheids in piñon and juniper are small compared to other conifers (Pittermann, Sperry, Hacke, et al., 2006; Sperry, Hacke, & Pittermann, 2006). The constraints of opposing design optima for hydraulic transport and safety may limit plasticity in earlywood tracheid anatomy, especially if the tracheids may be close to a minimum critical lumen size necessary for hydraulic function (Bouche et al., 2014).

Investigation of pit structure and function is the logical next step to understand the dramatic differences in transport and safety between piñon and juniper xylems. Pit membrane size (i.e., margo size if torus size remains constant) has been shown to respond to drought stress in piñon (Gaylord, Kolb, & McDowell, 2015), with drought stressed trees producing tracheids with smaller pit membranes. Reduced margo area diminishes flow between adjacent tracheids and may account for the reduced K_S values measured in droughted trees. Though margo porosity is not linked to embolism vulnerability (Bouche et al., 2014), emboli propagate via pit connections, so pit structure and function may directly inform embolism vulnerability (Bouche et al., 2014; Zelinka et al., 2015). The degree to which the torus overlaps the pit aperture determines the magnitude of pressure difference necessary to promote embolism spread (Bouche et al., 2014). Members of the genus *Pinus* have thin, flat, disc-shaped tori, whereas *Juniperus* species have thick, convex, lens-shaped tori (Bauch, Liese, & Schultze, 1972). The more robust juniper torus may be more resistant to air seeding (Zelinka et al., 2015), and the combination of a more robust torus in a margo of equivalent porosity may explain the seemingly paradoxical result that juniper matches or exceeds piñon in both hydraulic efficiency and safety. Further investigation of the pit structure of these two species is necessary to test this hypothesis.

4.3 | Comparison of hydraulic function in current climate context

Although piñon and juniper did not exhibit the expected differences in hydraulic architecture, their patterns of function were consistent with the well-established functional differences between the study species (Limousin et al., 2013; Linton et al., 1998; McDowell et al., 2008; Pangle et al., 2015; Plaut et al., 2012; West et al., 2007). Under ambient conditions, higher A_S:A_L allowed piñon to compensate for lower K_S and to maintain an equivalent K_L and E_b to juniper. Postmonsoon $\Delta\Psi$ was similar in both species such that differences in leaf level processes (i.e., stomatal or mesophyll conductance) should be responsible for differences in gas exchange and carbon capture between piñon and juniper when water is available. As soil moisture decreased, the characteristic differences in embolism vulnerability and stomatal regulation between piñon and juniper produced very different functional responses. The relationship between E_b and Ψ_{PD} predicted anisohydric juniper to continue transpiration to drier soil conditions, and isohydric

piñon to cease transpiration at relatively modest values of water stress (Figure 6c). The values of $\Psi_{E=0}$ we calculated (−2.34 MPa for piñon and −4.89 MPa for juniper) correspond with observations of Ψ_{PD} of zero assimilation from studies on piñon/juniper leaf-level gas exchange: D. G. Williams and Ehleringer (2000) reported −2.0 MPa for piñon sampled across a latitudinal gradient spanning central Arizona to northern Utah; Lajtha and Barnes (1991) reported −2.2 MPa for piñon and −4.6 MPa for juniper from northern New Mexico; and Limousin et al. (2013) reported −2.55 MPa for piñon and −4.94 to −6.90 MPa for juniper from the same population of target trees measured in this study. Our shoot hydraulic estimates of E_b were consistent with reported values of leaf-level gas exchange (stomatal conductance) for piñon and juniper in the literature (Garcia-Forner et al., 2016, Limousin et al., 2013). Direct measurement of gas exchange at the leaf level has the advantage of integrating the various conductances along the soil–plant–atmosphere hydraulic path and incorporates the complex dynamics of water transport in both roots and leaves. We do not suggest that our calculations of E_b supplant leaf-level gas exchange measurements, but that our data are complimentary to these direct measurements. Our methods provide insight to performance in a low resistance portion of the plant hydraulic path length, and differences between branch hydraulics calculated transpiration rates and measured transpiration rates might elucidate the magnitude of leaf-specific hydraulic resistances on gas exchange.

4.4 | Functional consequences of isoshydry versus anisohydry

Our estimates of $\Psi_{E=0}$ support the hypothesis that plants sacrifice transpiration and carbon capture to preserve xylem hydraulic integrity (Cochard & Delzon, 2013; Sperry, 2000; Tyree & Sperry, 1989). In both species, Ψ_W rarely exceeded P_e and then only by small margins (Figure 9, though in the extremely dry premonsoon sampling of 2011, water potentials from ambient piñon predicted ~40% PLC). This indicates that both species generally employ an embolism avoidance strategy by closing stomata and limiting gas exchange as plant water status approaches P_e (Domec et al., 2008; Meinzer et al., 2009, Martínez-Vilalta et al., 2014). Juniper had a larger absolute difference between $\Psi_{E=0}$ and P_e than piñon (0.77 vs. 0.24 MPa), but the relative magnitudes of the differences for both species were similar (P_e was 14.9% greater than $\Psi_{E=0}$ in juniper and 9.9% greater in piñon).

Although our results do not challenge the isohydric/anisohydric labels of piñon and juniper, both species appear to have similar relative risks for embolism (Figure 9), despite their disparate positions on the continuum from isohydric to anisohydric stomatal regulation (Klein, 2014). However, because piñon operated within a more restricted range of water potentials, we observed piñon exhibiting Ψ_W values in excess of P_e more frequently than juniper. Our predictions of PLC are thus consistent with other studies (Garcia-Forner et al., 2016, McDowell et al., 2013; Plaut et al., 2012) that found piñon was more likely to experience significantly greater PLC compared to juniper, with surviving piñon enduring approximately 45% PLC, whereas juniper PLC stayed below 15%. Slight differences in reported values of Weibull fit parameters from vulnerability curves and measured Ψ_{MD} produced different estimates of PLC across studies but do not negate the conclusion that isohydric piñon suffers greater loss of hydraulic function than anisohydric juniper. This refutes the hypothesis that isohydric species should be less prone to embolism and hydraulic failure (per McDowell et al., 2008 and Skelton et al., 2015). It is noteworthy that our study, as well as that of Garcia-Forner et al. (2016), investigated trees that survived drought. PLC was observed to be significantly higher in these same species (and at the same site as this study) for trees that died (McDowell et al., 2013), in line with strong evidence that prolonged, elevated PLC promotes mortality (cf. Anderegg et al., 2015).

4.5 | Implications for predicted future climate scenarios

Our results suggest piñon will be more susceptible to local extirpation than juniper in projected climate scenarios for the semiarid southwestern US (McDowell et al., 2015; Seager et al., 2007; Williams et al., 2013), as juniper matched or out-performed piñon in every hydraulic metric we measured. Though juniper did not demonstrate major adjustments in xylem structure or function, more negative $\Psi_{E=0}$ and P_e should confer an enhanced likelihood of survival in the novel climate space generated if temperatures rise and precipitation inputs become smaller and/or less frequent across the semiarid southwestern US, as predicted by future climate models (Seager et al., 2007; Seager, Vecchi, & MacDonald, 2010; Williams et al., 2013). Increased aridity, as a function of enhanced atmospheric demand combined with reduced soil moisture pools, will impose more strict limits on carbon capture by both species (McDowell et al., 2015). Both piñon-juniper woodlands and juniper savannas currently function as net carbon sinks, but sink strength in both of these systems is predicted to diminish with increasing temperature and/or reduced precipitation (Anderson-Teixeira, Delong, Fox, Brese, & Litvak, 2011; Biederman et al., 2016). Piñon mortality will exacerbate loss of ecosystem sink strength (Bonan, 2008; Reichstein et al., 2014), especially if mass mortality occurs over the entire piñon–juniper range and have serious implications for terrestrial–atmosphere carbon balance over a significant portion of southwestern US vegetated landscapes (Krofcheck et al., 2016). Thus, mass piñon mortality will contribute to an increasingly challenging climate for surviving piñon. Absent the ability to produce more drought-resistant xylem needed to extract water from drier soils or maintain positive $\Delta\Psi$ over more negative Ψ_{soil} conditions, piñon are unlikely to maintain gas exchange, and the positive carbon balance necessary to meet growth, maintenance, and defense demands in a hotter, drier southwestern US.

ACKNOWLEDGEMENTS

Judson Hill, Enrico Yepez, Jen Plaut, Clif Meyer, Renee Brown, James Elliot, and many undergraduate assistants were essential in establishing this experiment. Ben Specter, Katie Sauer, Laura Pickrell, and Kelsey Flathers provided excellent field assistance. This research was supported by the U.S. Department of Energy's Office of Science (BER) awards to NGM and WTP, with additional support from the National Science Foundation via the Sevilleta LTER (NSF DEB-0620482) and the Sevilleta summer graduate fellowship to PJH. The authors herein state that they have no conflict of interest declare.

ORCID

P. J. Hudson http://orcid.org/0000-0001-7759-2321

REFERENCES

Alder, N. N., Sperry, J. S., & Pockman, W. T. (1996). Root and stem xylem embolism, stomatal conductance, and leaf turgor in *Acer grandidentatum* populations along a soil moisture gradient. *Oecologia*, *105*, 293–301.

Anderegg, W. R. L., Flint, A., Huang, C.-Y., Flint, L., Berry, J. A., Davis, F. W., &Field, C. B., (2015). Tree mortality predicted from drought-induced vascular damage. *Nature Geoscience*, *8*, 367–371.

Anderson-Teixeira, K. J., Delong, J. P., Fox, A. M., Brese, D. A., & Litvak, M. E. (2011). Differential responses of production and respiration to temperature and moisture drive the carbon balance across a climatic gradient in New Mexico. *Global Change Biology*, *17*, 410–424.

Awad, H., Barigah, T., Badel, E., Cochard, H., & Herbette, S. (2010). Poplar vulnerability to xylem cavitation acclimates to drier soil conditions. *Physiologia Plantarum*, *139*, 280–288.

Barnard, D. M., Meinzer, F. C., Lachenbruch, B., McCulloh, K. A., Johnson, D. M., & Woodruff, D. R. (2011). Climate-related trends in sapwood biophysical properties in two conifers: Avoidance of hydraulic dysfunction through coordinated adjustments in xylem efficiency, safety and capacitance. *Plant, Cell & Environment*, *34*, 643–654.

Bates, D. M., Maechler, M., & Bolker, B. (2012). lme4: Linearmixed-effects models using S4 classes. R package version 0.999999-0.

Bauch, J. W., Liese, W., & Schultze, R. (1972). The morphological variability of the bordered pit membranes in gymnosperms. *Wood Science and Technology*, *6*, 165–184.

Beikircher, B., & Mayr, S. (2009). Intraspecific differences in drought tolerance and acclimation in hydraulics of *Ligustrum vulgare* and *Viburnum lantana*. *Tree Physiology*, *29*, 765–775.

Biederman, J. A., Scott, R. L., Goulden, M. L., Vargas, R., Litvak, M. E., Kolb, T. E., … Burns, S. P., (2016). Terrestrial carbon balance in a drier world: The effects of water availability in southwestern North America. *Global Change Biology*, *22*, 1867–1879.

Bonan, G. B. (2008). Forests and climate change: Forcings, feedbacks, and the climate benefits of forests. *Science*, *320*, 1444–1449.

Bouche, P. S., Larter, M., Domec, J. C., Burlett, R., Gasson, P., Jansen, S., & Delzon, S. (2014). A broad survey of hydraulic and mechanical safety in the xylem of conifers. *Journal of Experimental Botany*, *65*, 4419–4431.

Breshears, D. D., Myers, O. B., Meyer, C. W., Barnes, F. J., Zou, C. B., Allen, C. D., … Pockman, W. T. (2009). Tree die-off in response to global change-type drought: Mortality insights from a decade of plant water potential measurements. *Frontiers in Ecology and the Environment*, *7*, 185–189.

Bryukhanova, M., & Fonti, P. (2012). Xylem plasticity allows rapid hydraulic adjustment to annual climatic variability. *Trees*, *27*, 485–496.

Bucci, S. J., Goldstein, G., Meinzer, F. C., Scholz, F. G., Franco, A. C., & Bustamante, M. (2004). Functional convergence in hydraulic architecture and water relations of tropical savanna trees: From leaf to whole plant. *Tree Physiology*, *24*, 891–899.

Choat, B., Jansen, S., Brodribb, T. J., Cochard, H., Delzon, S., Bhaskar, R., … Zanne, A. E. (2012). Global convergence in the vulnerability of forests to drought. *Nature*, *491*, 752–755.

Cochard, H., & Delzon, S. (2013). Hydraulic failure and repair are not routine in trees. *Annals of Forest Science*, *70*, 659–661.

Corcuera, L., Cochard, H., Gil-Pelegrin, E., & Notivol, E. (2011). Phenotypic plasticity in mesic populations of *Pinus pinaster* improves resistance to xylem embolism (P50) under severe drought. *Trees*, *25*, 1033–1042.

Domec, J. C., & Gartner, B. L. (2001). Cavitation and water storage capacity in bole xylem segments of mature and young Douglas-fir trees. *Trees*, *15*, 204–214.

Domec, J. C., & Gartner, B. L. (2002). How do water transport and water storage differ in coniferous earlywood and latewood? *Journal of Experimental Botany*, *53*, 2369–2379.

Domec, J. C., Lachenbruch, B., Meinzer, F. C., Woodruff, D. R., Warren, J. M., & McCulloh, K. A. (2008). Maximum height in a conifer is associated with conflicting requirements for xylem design. *Proceeding of the National Academy of Sciences of the United States*, *105*, 12069–12074.

Eilmann, B., Zweifel, R., Buchmann, N., Fonti, P., & Rigling, A. (2009). Drought-induced adaptation of the xylem in Scots pine and pubescent oak. *Tree Physiology*, *29*, 1011–1020.

Feild, T. S., Hudson, P. J., Balun, L., Chatelet, D. S., Patino, A. A., Sharma, C. A., & McLaren, K. (2011). The ecophysiology of xylem hydraulic constraints by "basal" vessels in *Canella winterana* (Canellaceae). *International Journal of Plant Sciences*, *172*, 879–888.

Fisher, R., McDowell, N., Purves, D.,Moorcroft, P.,Sitch, S.,Cox, P., … Woodward, F. I. (2010). Assessing uncertainties in a second-generation dynamic vegetation model caused by ecological scale limitations. *New Phytologist*, *187*, 666–681.

Fonti, P., & García-González, I. (2008). Earlywood vessel size of oak as a potential proxy for spring precipitation in mesic sites. *Journal of Biogeography*, *35*, 2249–2257.

Fonti, P., Heller, O., Cherubini, P., Rigling, A., & Arend, M. (2012). Wood anatomical responses of oak saplings exposed to air warming and soil drought. *Plant Biology*, *15*, 210–219.

Garcia-Forner, N., Adams, H. D., Sevanto, S.,Collins, A. D.,Dickman, L. T., Hudson, P. J., … McDowell, N. G. (2016). Responses of two semiarid conifer tree species to reduced precipitation and warming reveal new perspectives for stomatal regulation. *Plant, Cell & Environment*, *39*, 38–49.

Gaylord, M. L., Kolb, T. E., & McDowell, N. G. (2015). Mechanisms of piñon pine mortality after severe drought: A retrospective study of mature trees. *Tree Physiology*, *35*, 806–816.

Gleason, S. M., Westoby, M., Jansen, S.,Choat, B.,Hacke, U. G.,Pratt, R. B., … Zanne, A. E. (2015). Weak tradeoff between xylem safety and xylem-specific hydraulic efficiency across the world's woody plant species. *New Phytologist*, *209*, 123–136.

Grier, C. G., & Running, S. W. (1977). Leaf area of mature northwestern coniferous forests: Relation to site water balance. *Ecology*, *58*, 893–899.

Hacke, U. G., & Jansen, S. (2009). Embolism resistance of three boreal conifer species varies with pit structure. *New Phytologist*, *182*, 675–686.

Hacke, U. G., Sperry, J. S., & Pittermann, J. (2004). Analysis of circular bordered pit function II. Gymnosperm tracheids with torus-margo pit membranes. *American Journal of Botany*, *91*, 386–400.

Hacke, U. G., Sperry, J. S., Pockman, W. T., Davis, S. D., & McCulloh, K. A. (2001). Trends in wood density and structure are linked to prevention of xylem implosion by negative pressure. *Oecologia*, *126*, 457–461.

Herbette, S., Wortemann, R., Awad, H., Huc, R., Cochard, H., & Barigah, T. S. (2010). Insights into xylem vulnerability to cavitation in *Fagus sylvatica* L.: Phenotypic and environmental sources of variability. *Tree Physiology*, *30*, 1448–1455.

Hsiao, T. C., & Acevedo, E. (1974). Plant responses to water deficits, water-use efficiency, and drought resistance. *Agricultural Meteorology*, *14*, 59–84.

Hubbard, R. M., Ryan, M. G., Stiller, V., & Sperry, J. S. (2001). Stomatal conductance and photosynthesis vary linearly with plant hydraulic conductance in ponderosa pine. *Plant, Cell and Environment*, *24*, 112–121.

Hudson, P. J., Razanatsoa, J., & Feild, T. S. (2009). Early vessel evolution and the diverisification of wood function: Insights from Malagasy Canellales. *American Journal of Botany*, *97*, 80–93.

Klein, T. (2014). The variability of stomatal sensitivity to leaf water potential across tree species indicates a continuum between isohydric and anisohydric behaviours. *Functional Ecology*, *28*, 1313–1320.

Klein, T., Di Matteo, G., Rotenberg, E., Cohen, S., & Yakir, D. (2013). Differential ecophysiological response of a major Mediterranean pine species across a climatic gradient. *Tree Physiology*, *33*, 26–36.

Krofcheck, D., Eitel, J., Lippitt, C., Vierling, L., Schulthess, U., & Litvak, M. (2016). Remote sensing based simple models of GPP in both disturbed and undisturbed Piñon-Juniper woodlands in the Southwestern U.S. *Remote Sensing*, *8*, 20. https://doi.org/10.3390/rs8010020.

Ladjal, M., Huc, R., & Ducrey, M. (2005). Drought effects on hydraulic conductivity and xylem vulnerability to embolism in diverse species and provenances of Mediterranean cedars. *Tree Physiology*, *25*, 1109–1117.

Lajtha, K., & Barnes, F. J. (1991). Carbon gain and water use in pinyon pine-juniper woodlands of northern New Mexico: Field versus phytotron chamber measurements. *Tree Physiology*, *9*, 59–67.

Lamy, J. B., Bouffier, L., Burlett, R., Plomion, C., Cochard, H., & Delzon, S. (2011). Uniform selection as a primary force reducing population genetic differentiation of cavitation resistance across a species range. *PLoS One*, *6*, e23476. https://doi.org/10.1371/journal.pone.0023476.s003.

Lamy, J. B., Delzon, S., Bouche, P. S., Alia, R., Vendramin, G. G., Cochard, H., & Plomion, C. (2013). Limited genetic variability and phenotypic plasticity detected for cavitation resistance in a Mediterranean pine. *New Phytologist*, *201*, 874–886.

Limousin, J., Bickford, C. P., Dickman, L. T., Pangle, R., E., Hudson, P. J., Boutz, A. L., … McDowell, N. G. (2013). Regulation and acclimation of leaf gas exchange in a piñon–juniper woodland exposed to three different precipitation regimes. *Plant, Cell & Environment*, *36*, 1812–1825.

Linton, M. J., Sperry, J. S., & Williams, D. G. (1998). Limits to water transport in *Juniperus osteosperma* and *Pinus edulis*: Implications for drought tolerance and regulation of transpiration. *Functional Ecology*, *12*, 906–911.

Maherali, H., & DeLucia, E. H. (2000). Xylem conductivity and vulnerability to cavitation of ponderosa pine growing in contrasting climates. *Tree Physiology*, *20*, 859–867.

Maherali, H., Pockman, W. T., & Jackson, R. B. (2004). Adaptive variation in the vulnerability of woody plants to xylem cavitation. *Ecology*, *85*, 2184–2199.

Manzoni, S., Vico, G., Katul, G., Palmroth, S., Jackson, R. B., & Porporato, A. (2013). Hydraulic limits on maximum plant transpiration and the emergence of the safety-efficiency trade-off. *New Phytologist*, *198*, 169–178.

Martin-StPaul, N. K., Limousin, J. M., Vogt-Schilb, H., Rodríguez-Calcerrada, J., Rambal, S, Longepierre, D., & Misson, L. (2013). The temporal response to drought in a Mediterranean evergreen tree: comparing a regional precipitation gradient and a throughfall exclusion experiment. *Global Change Biology*. https://doi.org/10.1111/gcb.12215

Martínez-Vilalta, J., Cochard, H., Mencuccini, M.,Sterck, F.,Herrero, A., Korhonen, J. F. L., … Zweifel, R. (2009). Hydraulic adjustment of scots pine across Europe. *New Phytologist*, *184*, 353–364.

Martínez-Vilalta, J., & Piñol, J. (2002). Drought-induced mortality and hydraulic architecture in pine populations of the NE Iberian Peninsula. *Forest Ecology and Management*, *161*, 247–256.

Martínez-Vilalta, J., Poyatos, R., Aguadé, D., Retana, J., & Mencuccini, M. (2014). A new look at water transport regulation in plants. *New Phytologist*, *204*, 105–115.

McCulloh, K. A., Johnson, D. M., Meinzer, F. C., & Woodruff, D. R. (2014). The dynamic pipeline: Hydraulic capacitance and xylem hydraulic safety in four tall conifer species. *Plant, Cell & Environment*, *37*, 1171–1183.

McDowell, N. G. (2011). Mechanisms linking drought, hydraulics, carbon metabolism, and vegetation mortality. *Plant Physiology*, *155*, 1051–1059.

McDowell, N. G., Adams, H. D., Bailey, J. D., Hess, M., & Kolb, T. E. (2006). Homeostatic maintenance of ponderosa pine gas exchange in response to stand density changes. *Ecological Applications: a Publication of the Ecological Society of America*, *16*, 1164–1182.

McDowell, N. G., Fisher, R. A., Xu, C., Domec, J. C., Hölttä, T., Mackay, D. S., … Pockman, W. T. (2013). Evaluating theories of drought-induced vegetation mortality using a multimodel-experiment framework. *New Phytologist*, *200*, 304–321.

McDowell, N., Pockman, W. T., Allen, C. D., Breshears, D. D., Cobb, N., Kolb, T., … Yepez, E. A. (2008). Mechanisms of plant survival and mortality during drought: Why do some plants survive while others succumb to drought? *New Phytologist*, *178*, 719–739.

Martínez-Vilalta, J., Cochard, H., Mencuccini, M.,Sterck, F.,Herrero, A., Korhonen, J. F. L., … Zweifel, R. (2015). Multi-scale predictions of massive conifer mortality due to chronic temperature rise. *Nature Climate Change*, *6*, 295–300.

McMahon, S. M., Harrison, S. P., Armbruster, W. S., Bartlein, P. J., Beale, C. M., Edwards, M. E., … Prentice, I. C. (2011). Improving assessment and modeling of climate change impacts on global terrestrial biodiversity. *Trends in Ecology & Evolution*, *26*, 249–259.

Medeiros, J. S., & Pockman, W. T. (2011). Drought increases freezing tolerance of both leaves and xylem of *Larrea tridentata*. *Plant, Cell & Environment*, *34*, 43–51.

Meinzer, F. C., Johnson, D. M., Lachenbruch, B., McCulloh, K. A., & Woodruff, D. R. (2009). Xylem hydraulic safety margins in woody plants: Coordination of stomatal control of xylem tension with hydraulic capacitance. *Functional Ecology*, *23*, 922–930.

Meinzer, F. C., Woodruff, D. R., Domec, J. C., Goldstein, G., Campanello, P. I., Gatti, M. G., & Villalobos-Vega, R. (2008). Coordination of leaf and stem water transport properties in tropical forest trees. *Oecologia*, *156*, 31–41.

Mencuccini, M. (2003). The ecological significance of long-distance water transport: Short-term regulation, long-term acclimation and the hydraulic costs of stature across plant life forms. *Plant, Cell & Environment*, *26*, 163–182.

Mencuccini, M., & Comstock, J. (1997). Vulnerability to cavitation in populations of two desert species, Hymenoclea salsola and Ambrosia dumosa, from different climatic regions. *Journal of Experimental Botany*, *48*, 1323–1334.

Mencuccini, M., & Grace, J. (1994). Climate influences the leaf area/sapwood area ratio in Scots pine. *Tree Physiology*, *15*, 1–10.

Moore, D. I. (2014). Meteorology data at the Sevilleta National Wildlife Refuge, New Mexico, (1987–2014).

Nardini, A., Lo Gullo, M. A., & Salleo, S. (2011). Refilling embolized xylem conduits: Is it a matter of phloem unloading?. *Plant Science*, *180*, 604–611.

Neufeld, H. S., Grantz, D. A., Meinzer, F. C., Goldstein, G., Crisostos, G. M., & Crisostos, C. (1992). Genotypic variabilityin vulnerability of leaf xylem to cavitation in water-stressed and well-irrigated sugarcane. *Plant Physiology*, *100*, 1020–1028.

Oren, R., Sperry, J. S., Katul, G. G., Pataki, D. E., Ewers, B. E., Phillips, N., & Schäfer, K. V. R. (2002). Survey and synthesis of intra- and interspecific variation in stomatal sensitivity to vapour pressure deficit. *Plant, Cell & Environment*, *22*, 1515–1526.

Pangle, R. E., Hill, J. P., Plaut, J. A., Yepez, E. A., & Elliot, J. R. (2012). Methodology and performance of a rainfall manipulation experiment in a piñon-juniper woodland. *Ecosphere*, *3*, 1–20.

Pangle, R. E., Limousin, J. M., Plaut, J. A., Yepez, E. A., Hudson, P. J., Boutz, A. L., … McDowell, N. G. (2015). Prolonged experimental drought reduces plant hydraulic conductance and transpiration and increases mortality in a piñon-juniper woodland. *Ecology and Evolution*, *5*, 1618–1638.

Pinheiro, J., Bates, D., DebRoy, S., & Sarkar, D. (2016). nlme: Linear and Nonlinear Mixed Effects Models. R package version 3, 1–128.

Pittermann, J., Sperry, J. S., Hacke, U. G., Wheeler, J. K., & Sikkema, E. H. (2006). Inter-tracheid pitting and the hydraulic efficiency of conifer wood: The role of tracheid allometry and cavitation protection. *American Journal of Botany*, *93*, 1265–1273.

Pittermann, J., Sperry, J. S., Wheeler, J. K., Hacke, U. G., & Sikkema, E. H. (2006). Mechanical reinforcement of tracheids compromises the hydraulic efficiency of conifer xylem. *Plant, Cell & Environment*, *29*, 1618–1628.

Plaut, J. A., Yepez, E. A., Hill, J., Pangle, R., Sperry, J. S., Pockman, W. T., & McDowell, N. G. (2012). Hydraulic limits preceding mortality in a piñon-juniper woodland under experimental drought. *Plant, Cell & Environment*, *35*, 1601–1617.

Plavcova, L., & Hacke, U. G. (2012). Phenotypic and developmental plasticitiy of xylem in hybrid poplar saplings subjected to experimental drought, nitrogen fertilization, and shading. *Journal of Experimental Botany*, *63*, 6481–6491.

Pockman, W. T., & McDowell, N. G. (2015). Ecosystem-scale rainfall manipulation in a Pinon-Juniper woodland: Tree sapwood and leaf area data (2011). *Long Term Ecological Research Network*. https://doi.org/10.6073/pasta/f4fbe653cd0a2b7bf645675fdc2294fa.

Pockman, W. T., & Sperry, J. S. (2000). Vulnerability to xylem cavitation and the distribution of Sonoran Desert vegetation. *American Journal of Botany*, *87*, 1287–1299.

R Development Core Team (2013). *R: A language and environment for statistical computing*. Vienna, Austria: R Foundation for Statistical Computing.

Reichstein, M., Bahn, M., Ciais, P., Frank, D., Mahecha, M. D., Senevirantne, S. I., … Wattenbach, M. (2014). Climate extremes and the carbon cycle. *Nature*, *500*, 287–295.

Seager, R., Ting, M., Held, I., Kushnir, Y., Lu, J., Vecchi, G., … Naik, N. (2007). Model projections of an imminent transition to a more arid climate in southwestern North America. *Science*, *316*, 1181–1184.

Seager, R., Vecchi, G. A., & MacDonald, G. M. (2010). Greenhouse warming and the 21st century hydroclimate of southwestern North America. *Proceedings of the National Academy of Sciences of the United States of America*, *107*, 21277–21282.

Sevanto, S. (2014). Phloem transport and drought. *Journal of Experimental Botany*, *65*, 1751–1759.

Sheffield, J., & Wood, E. F. (2007). Projected changes in drought occurrence under future global warming from multi-model, multi-scenario, IPCC AR4 simulations. *Climate Dynamics*, *31*, 79–105.

Sheriff, D. D., & Whitehead, D. (1984). Photosynthesis and wood structure in *Pinus radiata* during dehydration and immediately after rewatering. *Plant, Cell & Environment*, *7*, 53–62.

Skelton, R. P., West, A. G., & Dawson, T. E. (2015). Predicting plant vulnerability to drought in biodiverse regions using functional traits. *Proceedings of the National Academy of Sciences of the United States of America*, *112*, 5744–5749.

Sperry, J. S. (2000). Hydraulic constraints on plant gas exchange. *Agricultural and Forest Meteorology*, *104*, 13–23.

Sperry, J. S., & Hacke, U. G. (2004). Analysis of circular bordered pit function I. Angiosperm vessels with homogenous pit membranes. *American Journal of Botany*, *91*, 369–385.

Sperry, J. S., Hacke, U. G., & Pittermann, J. (2006). Size and function in conifer tracheids and angiosperm vessels. *American Journal of Botany*, *93*, 1490–1500.

Sperry, J. S., & Saliendra, N. Z. (1994). Intra-and inter-plant variation in xylem cavitation in *Betula occidentalis*. *Plant, Cell & Environment*, *17*, 1233–1241.

Sterck, F. J., Zweifel, R., Sass-Klaassen, U., & Chowdhury, Q. (2008). Persisting soil drought reduces leafspecific conductivity in Scots pine (Pinus sylvestris) and pubescent oak (Quercus pubescens). *Tree Physiology*, *28*, 529–536.

Stiller, V. (2009). Soil salinity and drought alter wood density and vulnerability to xylem cavitation of baldcypress (*Taxodium distichum* (L.) Rich.) seedlings. *Environmental and Experimental Botany*, *67*, 164–171.

Tyree, M. T., Davis, S. D., & Cochard, H. (1994). Biophysicalperspectives of xylem evolution: is there a trade-off of hydraulic efficiency for vulnerability to dysfunction? *International Journal of Wood Anatomists*, *15*, 335–360.

Tyree, M. T., & Ewer, F. W. (1991). The hydraulic architecture of trees and other woody plants. *New Phytologist*, *119*, 345–360.

Tyree, M. T., & Sperry, J. S. (1989). Vulnerability of xylem to cavitation and embolism. *Annual Review of Plant Physiology*, *40*, 19–38.

West, A. G., Hultine, K. R., Jackson, T. L., & Ehleringer, J. R. (2007). Differential summer water use by *Pinus edulis* and *Juniperus osteosperma* reflects contrasting hydraulic characteristics. *Tree Physiology*, *27*, 1711–1720.

Williams, A. P., Allen, C. D., Macalady, A. K., Griffin, D., Woodhouse, C. A., Meko, D. M., … McDowell, N. G. (2013). Temperature as a potent driver of regional forest drought stress and tree mortality. *Nature Climate Change*, *3*, 292–297.

Williams, D. G., & Ehleringer, J. R. (2000). Intra- and interspecific variation for summer precipitation use in Pinyon-Juniper woodlands. *Ecological Monographs*, *70*, 517–537.

Winter, B. (2013). Linear models and linear mixed effects models in R with linguistic applications. arXiv:1308.5499. [http://arxiv.org/pdf/1308.5499.pdf]

Wortemann, R., Herbette, S., Barigah, T. S., Fumanal, B., Alia, R., Ducousso, A., … Cochard, H. (2011). Genotypic variability and phenotypic plasticity of cavitation resistance in *Fagus sylvatica* L. across Europe. *Tree Physiology*, *31*, 1175–1182.

Wullschleger, S., Meinzer, F. C., & Vertessy, R. A. (1998). A review of whole-plant water use studies in trees. *Tree Physiology*, *18*, 499–512.

Zelinka, S. L., Bourne, K. J., Hermanson, J. C., Glass, S. V., Costa, A., & Wiedenhoeft, A. C. (2015). Force-displacement measurements of earlywood bordered pits using a mesomechanical tester. *Plant, Cell & Environment*, *38*, 2088–2097.

Zimmerman, M. H. (1983). *Xylem structure and the ascent of sap*. New York, NY, USA: Springer-Verlag.

Zweifel, R., Zimmermann, L., Zeugin, F., & Newbury, D. M. (2006). Intra-annual radialgrowth and water relations of trees: implications towards a growth mechanism. *Journal of Experimental Botany*, *57*, 1445–1459.

Zwieniecki, M. A., Melcher, P. J., & Holbrook, N. M. (2001). Hydrogel control of xylem hydraulic resistance in plants. *Science*, *291*, 1059–1062.

SUPPORTING INFORMATION

Additional Supporting Information may be found online in the supporting information tab for this article.

Table S1. Summary of the linear mixed models of the relationship between K_S and Ψ_{PD} for both species. K_S and Ψ_{PD} were used as response and explanatory variables, respectively, in both the piñon and juniper models.

Table S2. Summary of the linear mixed models of the relationship between K_L and Ψ_{PD} for both species. K_L and Ψ_{PD} were used as response and explanatory variables, respectively, for both juniper model and piñon models.

Table S3. Summary of the linear mixed models of the relationship between E_b and Ψ_{PD} for both species. E_b and Ψ_{PD} were used as response and explanatory variables, respectively, for both piñon and juniper models.

Figure S1. Relationships between predawn water potential (Ψ_{PD}) and midday water potential (Ψ_{MD}) for piñon (circles, dashed linear fit line) and juniper (squares, solid linear fit line) before and after monsoon onset (a,c). Dotted gray line indicates 1:1 scaling. Relationships between and driving gradient for piñon (circles, dashed linear fit line) and juniper (squares, solid linear fit line) before and after monsoon onset (b,d). Dotted gray line at $\Delta\Psi = 0$ indicates the point at which no driving gradient for transpiration exists.

How to cite this article: Hudson PJ, Limousin JM, Krofcheck DJ, et al. Impacts of long-term precipitation manipulation on hydraulic architecture and xylem anatomy of piñon and juniper in Southwest USA. *Plant Cell Environ*. 2018;41:421–435. https://doi.org/10.1111/pce.13109